Simulation of low clouds from the CAM and the regional WRF with multiple nested resolutions

Wuyin Lin,[1] Minghua Zhang,[1] and Jingbo Wu[2]

Received 31 December 2008; revised 13 March 2009; accepted 7 April 2009; published 29 April 2009.

[1] Current climate models have shown systematic simulation biases of low clouds that have cast great uncertainties on the climate sensitivity of these models. Among them is the deficient amount of low clouds over the storm tracks. This study uses the NCAR Community Atmospheric Model (CAM) and the Weather Research and Forecasting model (WRF) to study the cause of the failure of the global model in simulating low clouds associated with a frontal passage over the North Atlantic. The global model is shown to simulate the large-scale circulation that can support the boundary layer instabilities responsible for the observed clouds, but because the global model does not resolve the unstable modes, the instability cannot be realized. The resolution requirement of cloud simulations is discussed. This study also demonstrates the feasibility of cloud parameterization by nesting high resolution models into coarse resolution models to tap into the dynamical properties of the large-scale flows. **Citation:** Lin, W., M. Zhang, and J. Wu (2009), Simulation of low clouds from the CAM and the regional WRF with multiple nested resolutions, *Geophys. Res. Lett.*, *36*, L08813, doi:10.1029/2008GL037088.

1. Introduction

[2] Low clouds have the largest net radiative effects on the Earth-atmosphere system because of their large impact on solar radiation but relatively small impact on infrared radiation. These clouds are also believed to be responsible for the large discrepancies of cloud feedbacks and the sensitivities of climate models [*Bony and Dufresne*, 2005; *Dufresne and Bony*, 2008]. Aside from the climate feedback problem, low clouds are also intimately connected to boundary layer turbulences and pollution dispersions.

[3] Several studies have shown however that GCMs systematically underestimate low clouds over the globe [*Webb et al.*, 2001; *Tselioudis and Jakob*, 2002; *Lin and Zhang*, 2004; *Zhang et al.*, 2005].

[4] This study focuses on one of the regions where low clouds are often significantly underestimated in GCMs over the mid-latitude storm tracks. We aim to answer the following two questions: (1) What levels of sophistication of numerical models are needed to simulate the observed low clouds in this region? (2) Are biases in GCMs caused by deficiencies in large-scale circulation or by missing physics?

[5] The objective of the present study is to understand the causes of deficient low clouds in GCMs and to improve the global models. The investigation is carried out by using both the NCAR Community Climate Model (CAM3.1) and the Weather Research and Forecasting Model (WRF2.0) with successively higher spatial resolutions, and through a case study. To our knowledge, this is the first study to use regional models up to cloud-resolving scales to evaluate physical processes of low clouds in GCMs.

[6] We will show that the large-scale atmospheric dynamic and thermodynamic conditions in the GCM meet all the instability criteria of boundary layer flows. But since the modes of instability cannot be resolved in the large-scale models, the instability cannot be materialized, and thus no clouds in the GCM.

2. The Models and Case Description

[7] The global model is the NCAR CAM3.1 documented by *Collins et al.* [2006]. Low clouds in the model are calculated from three processes: stratiform clouds as a function of relative humidity, cumulus clouds as a function of convective mass flux, and inversion capped marine boundary layer clouds through the static stability relationship of *Klein and Hartmann* [1993]. The model uses T42 resolution with 26 layers in the vertical, four of which are below the altitude of the 850 mb level. The deficient amount of low clouds over the storm tracks in the model, particularly under conditions of synoptic subsidences has been reported by *Lin and Zhang* [2004].

[8] The regional model is the WRF2.0.3 described by *Michalakes et al.* [2005]. Clouds in WRF are diagnosed with either hundred or zero percentage for a grid box based on the presence of hydrometeors. The microphysics scheme used in our simulation is the six-class WRF Single Moment (WSM) scheme [*Hong et al.*, 2004], including water vapor, cloud water, cloud ice, rain, snow, and graupel.

[9] To compare with the global model simulation and observations, a set of WRF simulations with successively higher horizontal resolution are made with a grid spacing of 20, 7.2, 6, 4, 2.4, 1.33 and 0.8 km. Except for 20 km, each high resolution model is nested within one or more coarser resolution models with a nesting ratio of three or five. Cumulus convective parameterization for resolutions of 6 km or higher is disabled. All WRF simulations have 30 vertical layers, with nine of them below the altitude of 850 mb.

[10] The case study focuses on low clouds associated with a cyclone passage over the north Atlantic on February 19, 2004. The sea level pressure and surface air temperature at 15 UTC are overlaid on the satellite infrared image from GOES in Figure 1a, and the visible image is in Figure 1b.

[1]School of Marine and Atmospheric Sciences, Stony Brook University, State University of New York, Stony Brook, New York, USA.
[2]NASA GISS, Columbia University, New York, New York, USA.

0094-8276/09/2008GL037088$05.00

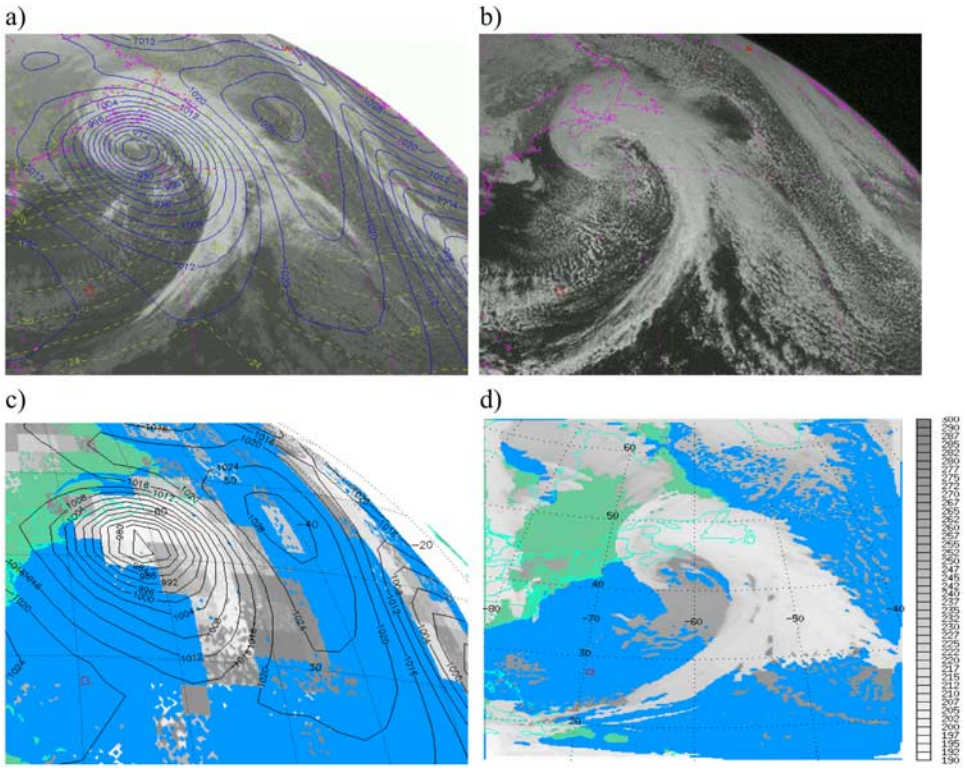

Figure 1. Satellite and model cloud images at 15 UTC, Feb. 19, 2004. (a) Infrared image overlaid with sea level pressure (blue) and near surface air temperature (green) from GFS analysis. (b) Visible image. (c) CAM simulated cloud and sea level pressure, brighter color for higher cloud albedo. (d) WRF 20 km model simulated clouds, brighter color for higher cloud tops. The red box marks the location for high resolution WRF simulations and further analyses.

The cyclone is associated with a typical comma-head cloud shield along the cold front and to the northeast of the surface cyclone. Behind the front, there is a large-area of low clouds that are more prominent in the visible image than in the infrared image due to their lower altitude but large optical depth. These low clouds are formed over regions of large cold advections and display features of cloud streets, cellular structures, and irregular shapes. Using satellite data, *Bakan and Schwarz* [1992] showed that these clouds can account for a significant percentage of low clouds in the winter storm tracks.

3. Simulation Results

[11] Clouds and surface pressure simulated in the CAM and WRF with 20 km resolution are shown in Figures 1c and 1d, respectively. Both the global CAM and the regional WRF are initialized at 00 UTC on February 18, 2004 by using the NCEP GFS analysis. For the WRF, lateral boundary forcing is prescribed with GFS analysis. The initialization procedure of the CAM was described by *Wu et al.* [2007] which used direct mapping and interpolation of the analysis fields to CAM grids.

[12] Both the location and the intensity of the cyclone are well captured in the models. The CAM however only simulates the cloud shield ahead of the cold front where large-scale upward motion exists. No clouds are simulated behind the cold front. Since these clouds can contribute up to 20% of low clouds over the storm tracks, they contribute to the overall deficient amount of low clouds in the CAM. The WRF simulates better the patterns of the frontal clouds, including the comma-head shape. The WRF however also underestimates a significant amount of low clouds behind the front.

[13] We next carry out simulations using the WRF with higher resolution nested within coarse resolution models. Figure 2a shows a simulation in which a 7.2 km resolution WRF is nested behind the front within a 36 km resolution WRF. More low clouds are simulated in the nested domain, but clouds are still missing around the area highlighted by a red box. When a higher resolution of WRF is further nested near the highlighted area, Figure 2b shows that more clouds are simulated.

[14] There is an indication of convergence of cloud amount when the resolution is finer than 4 km. Cloud distribution for the 0.8 km resolution domain, a size about 64 km by 64 km, is shown in Figure 2c. A distinctive feature is the cloud streets to the north of the simulation domain as commonly observed. Figure 2d shows the same cloud distribution within the nested 2.4 km and 0.8 km resolution domains. A remarkable continuity is seen across the boundary of the models with two different resolutions, suggesting convergence of cloud properties with the resolutions.

[15] This convergence can be also seen in Figure 3a which shows the area averaged cloud amount for the collocated domain of Figure 2c from various resolutions, and in Figure 3b which shows the cloud optical thickness. The simulated cloud amount and optical depth from the WRF with resolution equal to or higher than 4 km are

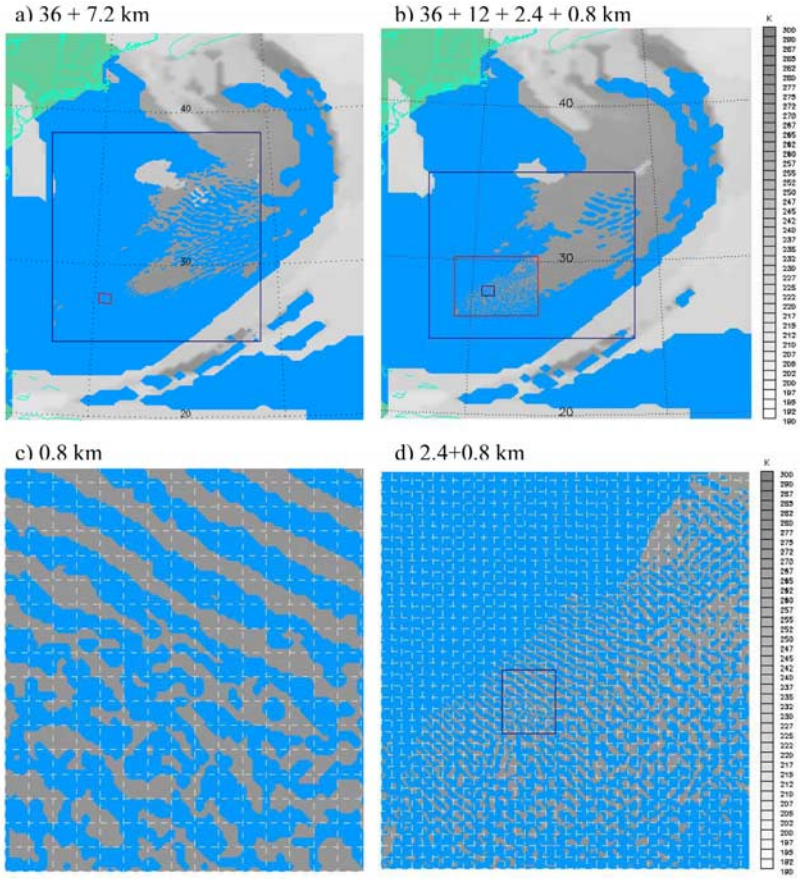

Figure 2. Contrast of WRF simulated clouds: (a) 36 + 7.2 km (the red box marks the location of the 0.8 km-resolution domain in Figure 2b); (b) 36 + 12 + 2.4 + 0.8 km; (c) the 0.8 km domain of Figure 2b with lines drawn every 5 grids; and (d) the two innermost domains of Figure 2b), i.e., 2.4 + 0.8 km.

similar to each other. At 7.2 km, no clouds are simulated. At 6 km resolution, optical depth is significantly less. A comparison of the optical depth from a MODIS http://modis-atmos.gsfc.nasa.gov) cloud scene in the region with a collocated simulation at 4 km resolution is shown in Figures 3c and 3d. Clouds in both the observation and simulation show considerable streak structures and share many similarities. But because the satellite cloud scene identification is different from that in the model, a more stringent comparison is not pursued.

4. Properties of Boundary-Layer Instability

[16] Formation of low clouds including cloud streets has been reviewed in several papers [*Brown*, 1980; *Atkinson and Zhang*, 1996; *Young et al.*, 2002]. The physical mechanisms can be broadly categorized into two groups. One is thermal convection under modulation of mean winds. When the stratification of the atmosphere is slightly unstable, roll circulation can develop as the optimal form of instability [e.g., *Kuo*, 1963; *Asai*, 1970]. The other is the dynamic instability of the Ekman flow in which the shear in the mean wind or the inflection of the wind that is perpendicular to the mean wind can result in roll instability [e.g., *Lilly*, 1966]. This dynamic instability can exist within neutrally stratified atmosphere.

[17] Atmospheric conditions such as in the present case are often with both thermal convection due to surface fluxes and shear of mean winds. The physical processes are also strongly influenced by capping inversion and wind-shear at the top of the boundary layer as well as radiative-driven turbulences from clouds. It is therefore often difficult to attribute low clouds to specific types of instabilities. Nevertheless, several non-dimensional parameters can be used to characterize the large-scale environment in which cloud streets can form [*LeMone*, 1973; *Moeng and Sullivan*, 1994]. These are the Richardson number, the Reynolds number, and the relative magnitudes of the friction velocity to the convective velocity in the boundary layer. The latter is also equivalent to the ratio of the boundary layer depth to the Monin-Obukhov length.

[18] Our premise is that if the values of these non-dimensional parameters in the coarse resolution model (GCM) are the same as those in the high-resolution models, the atmospheric large-scale dynamic and thermodynamic conditions in the GCM then possess the instability property to support the development of clouds. The reason why clouds are not simulated is then due to the inability of the model to materialize the instability. If the non-dimensional parameters are different between coarse and high resolution models, the large-scale circulation of the GCM then needs to be improved.

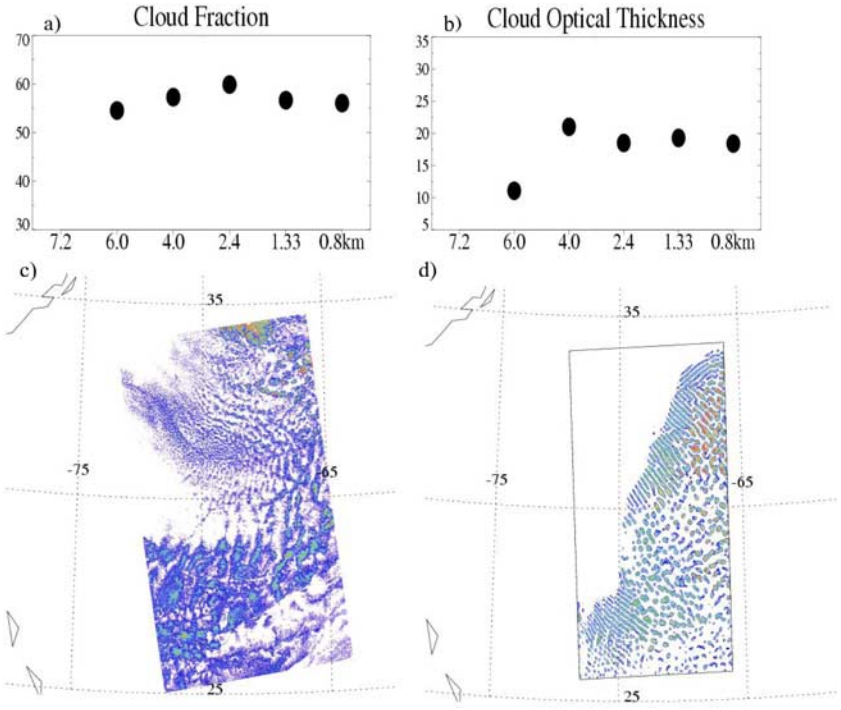

Figure 3. Cloud fraction and cloud optical thickness. (a) WRF simulated cloud fraction for the collocated domain shown in Figure 2c as a function of horizontal resolution. Each is from the innermost domain of separate simulations. (b) Same as Figure 3a except for in-cloud cloud optical thickness. (c) Cloud optical thickness from a MODIS L2 granule at 18 UTC, Feb. 19, 2004, warmer color for higher values. (d) Cloud optical thickness from the WRF 4 km resolution domain (in a nested simulation of 36 + 12 + 4 km).

[19] The boundary layer bulk Richardson number is used here and calculated as

$$R_i = g\delta(\theta_{vi} - \theta_s)/\overline{\theta_v}V_g^2$$

where δ is the boundary layer height, θ_s the surface air potential temperature, θ_{vi} the virtual potential temperature at δ and $\overline{\theta_v}$ the mean in the boundary layer. V_g is the geostrophic wind at the top of the boundary layer. Previous theoretical analysis showed that roll convection develops when $0 > Ri > -2.0$ [*Kuo*, 1963]. Figure 4a shows *Ri* for the collocated domain of Figure 2c as a function of different model resolutions. It is seen that values of *Ri* in both CAM and WRF are within the range of roll convection.

[20] The boundary layer Reynolds number is calculated as

$$R_e = \frac{2V_g}{f\delta}$$

in which f is the Coriolis parameter. This parameter measures the instability due to wind shear and inflection in the boundary layer. A value larger than 55 but less than 300 corresponds to parallel instability and a value larger than 300 corresponds to inflectional instability [*Lilly*, 1966; *LeMone*, 1973]. Figure 4b shows *Re* in the CAM and in the WRF with different horizontal resolutions. All values are within a single range of instability regime between 55 and 300.

[21] The friction and convective velocities as defined below

$$u^* = \left(\overline{u'w'}^2 + \overline{v'w'}^2\right)^{1/4}$$

$$w^* = \left[\frac{g\left(\overline{w'\theta_v'}\right)_0}{\theta_v} \times \delta\right]^{1/3},$$

are calculated in the WRF at each grid before being averaged over the 64 km by 64 km domain. In the CAM, these velocity scales are directly taken from the parameterizations. *Moeng and Sullivan* [1994] used the ratio of u*/w* as a criterion of cloud streets, but they pointed out that the threshold ratio is likely affected by capping inversion and other factors. Figures 4c and 4d show the two velocity scales in all simulations. They are in good agreement with each other.

[22] We therefore come to the conclusion that the large-scale environmental conditions that control the development of low clouds in the present case are similar in all versions of the models. These conditions are shown to have the attributes to support the thermal and dynamic instabilities to favor the formation of cloud streets. The instabilities however cannot be realized in coarse resolution models including the CAM and WRF-20 km because the unstable modes of the circulations responsible for the low clouds are not resolved in the models. This is different from the circum-

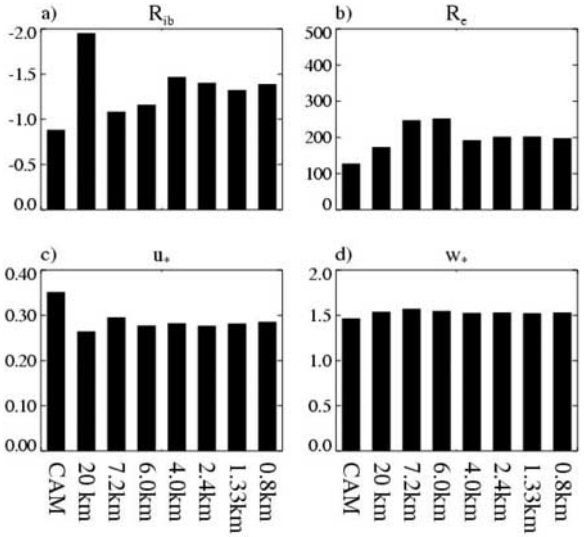

Figure 4. PBL parameters as a function of models (CAM and WRF at different resolutions): (a) boundary layer bulk Richardson number, (b) PBL Reynolds number, (c) friction velocity, and (d) convective velocity.

stances in which the controlling dynamic and thermodynamic conditions of clouds are missing in coarse resolution models even when the models are also initialized with operational analysis [*Katzfey and Ryan*, 2000; *Wu et al.*, 2007].

[23] Our simulation results in the previous section showed the convergence of cloud simulations with the WRF when the resolution is higher than 4 km. The above discussion on flow instability suggests that this conclusion is likely dependent on cloud types. In the present study, the horizontal wavelength of cloud streets in the traverse direction as shown in Figure 2c is close to 10 km. This barely allows these waves to be resolved at 2.4 km resolution. Under more typical conditions, the aspect ratio of the most unstable modes of boundary flow (the ratio of horizontal to vertical scales) is between three to seven [*Young et al.*, 2002]. For a boundary layer height of 1.2 km as in the present study, the horizontal scale of the waves will be 4 to 8 km, which would then require a resolution closer to 0.8 km for the model solutions to converge.

5. Summary

[24] We have presented a case in which the global CAM failed to simulate low clouds behind a frontal system. This is consistent with the systematic biases of deficient amount of low clouds in climate models over the storm tracks. The regional model WRF with various resolutions is used to analyze the physical processes and the cause of the GCM bias.

[25] We showed that low clouds can be realistically simulated using the WRF with horizontal resolutions higher than 4 km, but not in coarser resolutions. Several non-dimensional parameters that control the formation of the simulated clouds are compared between the coarse and high resolution models. They are all in good agreement with each other. The failure of the coarse resolution model in simulating these low clouds is therefore attributed to the inability of these models to realize the small scale instability, rather than the large-scale conditions of the model atmosphere.

[26] Our study suggests that to simulate the low clouds associated with cold outbreaks, the spatial resolution of the model needs to be smaller enough to accommodate the most unstable modes of the atmospheric flow. Since the horizontal wavelength of these unstable modes is often only several times of the boundary layer height, the horizontal spatial resolution needs to be comparable to it, which is about 1 km.

[27] It would be a daunting task to try to parameterize these clouds. First, the dynamics of the unstable modes are impacted by radiative and microphysical processes of clouds. Second, the interactions of the mean profiles of the state variables and the parameterized large eddies need to be considered. Finally, the entraining of dry air from above the boundary layer is likely important, which is an unsolved problem itself.

[28] The results however point to the dynamical and physical processes that should be accounted for in cloud parameterizations. Our study also indicates the feasibility of nesting high resolution models within a large-scale model, which includes the use of multi-scale modeling framework (MMF), to sample regions of interest to simulate clouds. The parent model can provide the large-scale conditions, while the sub-domain model can be used to realize the instabilities of the large-scale flows.

[29] **Acknowledgments.** This research is supported under the NASA MAP program to Stony Brook University. Partial support is also from the DOE ARM and CCPP program and the National Science Foundation to Stony Brook University.

References

Asai, T. (1970), Three dimensional features of thermal convection in a pale Couette flow, *J. Meteorol. Soc. Jpn.*, *48*, 18–129.

Atkinson, B. W., and J. W. Zhang (1996), Mesoscale shallow convection in the atmosphere, *Rev. Geophys.*, *34*, 403–431.

Bakan, S., and E. Schwarz (1992), Cellular convection over the northeastern Atlantic, *Int. J. Climatol.*, *12*, 353–367.

Bony, S., and J.-L. Dufresne (2005), Marine boundary layer clouds at the heart of tropical cloud feedback uncertainties in climate models, *Geophys. Res. Lett.*, *32*, L20806, doi:10.1029/2005GL023851.

Brown, R. A. (1980), Longitudinal instabilities and secondary flows in the planetary boundary layer: A review, *Rev. Geophys.*, *18*, 683–697.

Collins, D. W., P. J. Rasch, B. A. Boville, J. J. Hack, J. R. McCaa, D. L. Williamson, B. P. Briegleb, C. M. Bitz, S.-J. Lin, and M. H. Zhang (2006), The formulation and atmospheric simulation of the Community Atmosphere Model: CAM3, *J. Clim.*, *19*, 2144–2161.

Dufresne, J. L., and S. Bony (2008), An assessment of the primary sources of spread of global warming estimates from coupled atmosphere-ocean models, *J. Clim.*, *21*, 5135–5144.

Hong, S.-Y., J. Dudhia, and S.-H. Chen (2004), A revised approach to ice microphysical processes for the bulk parameterization of clouds and precipitation, *Mon. Weather Rev.*, *132*, 103–120.

Katzfey, J. J., and B. F. Ryan (2000), Midlatitude frontal clouds: GCM-scale modeling implications, *J. Clim.*, *13*, 2729–2745.

Klein, S. A., and D. L. Hartmann (1993), The seasonal cycle of low stratiform clouds, *J. Clim.*, *6*, 1587–1606.

Kuo, H. L. (1963), Perturbations of plane Couette flow in stratified fluid and origin of cloud streets, *Phys. Fluids*, *6*, 195–211.

LeMone, M. (1973), The structure and dynamics of horizontal roll vortices in the PBL, *J. Atmos. Sci.*, *30*, 1077–1091.

Lilly, D. K. (1966), On the stability of Ekman boundary flow, *J. Atmos. Sci.*, *23*, 481–494.

Lin, W. Y., and M. H. Zhang (2004), Evaluation of clouds and their radiative effects simulated by the NCAR Community Atmospheric Model CAM2 against satellite observations, *J. Clim.*, *17*, 3302–3318.

Michalakes, J., J. Dudhia, D. Gill, T. Henderson, J. Klemp, W. Skamarock, and W. Wang (2005), The Weather Research and Forecast Model: Software architecture and performance, in *Use of High Performance*

Computing in Meteorology: Proceedings of the 11th ECMWF Workshop on the Use of High Performance Computing in Meteorology, edited by W. Zwieflhofer and G. Mozdzynski, pp. 156–168, World Sci., Singaore.

Moeng, C.-H., and P. P. Sullivan (1994), A comparison of shear- and buoyancy-driven planetary boundary layer flow, *J. Atmos. Sci.*, *51*, 999–1022.

Tselioudis, G., and C. Jakob (2002), Evaluation of midlatitude cloud properties in a weather and a climate model: Dependence on dynamic regime and spatial resolution, *J. Geophys. Res.*, *107*(D24), 4781, doi:10.1029/2002JD002259.

Webb, M., C. Senior, and S. Bony (2001), Combining ERBE and ISCCP data to assess clouds in the Hadley Centre, ECMWF and LMD atmospheric climate models, *Clim. Dyn.*, *17*, 905–922.

Wu, J., M. Zhang, and W. Lin (2007), A case study of a frontal system simulated by a climate model: Clouds and radiation, *J. Geophys. Res.*, *112*, D12201, doi:10.1029/2006JD008238.

Young, G. S., D. A. R. Kristovich, M. R. Hjelmfelt, and R. C. Foster (2002), Rolls, streets, waves, and more: A review of quasi-two-dimensional structures in the atmospheric boundary layer, *Bull. Am. Meteorol. Soc.*, *83*, 997–1001.

Zhang, M. H., et al. (2005), Comparing clouds and their seasonal variations in 10 atmospheric general circulation models with satellite measurements, *J. Geophys. Res.*, *110*, D15S02, doi:10.1029/2004JD005021.

W. Lin and M. Zhang, School of Marine and Atmospheric Sciences, Stony Brook University, State University of New York, Stony Brook, NY 11794-5000, USA. (wlin@atmsci.msrc.sunysb.edu)

J. Wu, NASA GISS, Columbia University, 2880 Broadway, New York, NY 10025, USA.